Temporal variations in meibomian gland structure—A pilot study

DOI:
10.1111/opo.13321

Document Version
Final published version

Received: 23 June 2023 | Accepted: 15 April 2024

DOI: 10.1111/opo.13321

OPO THE COLLEGE OF OPTOMETRISTS

ORIGINAL ARTICLE

Temporal variations in meibomian gland structure—A pilot study

Kasandra Swiderska[1] | **Caroline A. Blackie**[2] | **Carole Maldonado-Codina**[1] | **Martin Fergie**[3] | **Michael L. Read**[1] | **Philip B. Morgan**[1]

[1]Eurolens Research, Division of Pharmacy and Optometry, Faculty of Biology, Medicine and Health, The University of Manchester, Manchester, UK

[2]Johnson & Johnson Vision, Inc, Jacksonville, Florida, USA

[3]Division of Informatics, Imaging and Data Sciences, Faculty of Biology, Medicine and Health, The University of Manchester, Manchester, UK

Correspondence
Kasandra Swiderska, Eurolens Research, The University of Manchester, Manchester, UK.
Email: kasandra.swiderska@gmail.com

Funding information
Johnson and Johnson Vision, Inc., Grant/Award Number: R123302

Abstract

Purpose: To investigate whether there is a measurable change in meibomian gland morphological characteristics over the course of a day (12 h) and over a month.

Methods: The study enrolled 15 participants who attended a total of 11 study visits spanning a 5-week period. To assess diurnal changes in meibomian glands, seven visits were conducted on a single day, each 2 h apart. For monthly assessment, participants attended an additional visit at the same time of the day every week for three consecutive weeks. Meibography using the LipiView® II system was performed at each visit, and meibomian gland morphological parameters were calculated using custom semi-automated software. Specifically, six central glands were analysed for gland length ratio, gland width, gland area, gland intensity and gland tortuosity.

Results: The average meibomian gland morphological metrics did not exhibit significant changes during the course of a day or over a month. Nonetheless, certain individual gland metrics demonstrated notable variation over time, both diurnally and monthly. Specifically, meibomian gland length ratio, area, width and tortuosity exhibited significant changes both diurnally and monthly when assessed on a gland-by-gland basis.

Conclusions: Meibomian glands demonstrated measurable structural change over short periods of time (hours and days). These results have implications for innovation in gland imaging and for developing precision monitoring of gland structure to assess meibomian gland health more accurately.

KEYWORDS
meibography, meibomian gland function, meibomian gland imaging, meibomian gland structure, meibomian glands

INTRODUCTION

Existing clinically accessible methods of meibomian gland imaging are predominantly intended to capture data from a single time point, with the assumption that visible gland structure changes very slowly over time. No previous work has assessed the potential for 'normal' and likely subtle morphological changes in meibomian glands over relatively short time periods (hours and days). Despite previous work assessing the potential to relate meibomian gland structure with function,[1–5] little is known about the possibility of interpreting gland function directly from images of gland structure. This seems a reasonable area of exploration given the holocrine nature of meibomian glands, where there is an inherent overlap between structure and function.

Meibomian gland structure is typically used to indicate the severity and progress of meibomian gland dysfunction

(MGD) and also to inform the likelihood of treatment success.[6] While it is known that gland function is compromised when gland complete dropout occurs, further exploration is needed to understand what additional and meaningful information can be gleaned from more detailed meibomian gland structural metrics. Additional studies are needed to elucidate the specific structural changes that affect gland function, such as alterations in gland acini size, ductal width or gland tortuosity, and how these changes can be best detected and accurately monitored.

Examining the diurnal variation in meibomian gland structure has the potential to provide insight into the subtleties of the healthy state as well as early indication of disease. Just as gland presence in no way guarantees gland function, gland absence may not indicate gland loss. Gland absence could be an indicator of altered acini activity, an accumulation of keratinised cells or neither of these phenomena.[1,7] These unknowns regarding gland structure, including short-term gland variability, have implications for patient prognosis and treatment recommendations and diagnostic and treatment innovations. Investigating the diurnal variation in meibomian gland structure and establishing methods to assess and evaluate a variety of structural characteristics in healthy individuals is a meaningful step to address some of these unknowns.

MGD is a common condition that affects a significant portion of the population and is considered a leading cause of associated dry eye disease.[8] MGD is characterised by structural and functional changes in the meibomian glands, including gland atrophy, fibrosis, obstruction and altered meibum composition.[9] Where meibomian gland atrophy has been considered irreversible in the past, recent studies have demonstrated that treatments such as vectored thermal pulsation and topical diquafosol therapy can improve gland structure.[2–4] Moreover, the evidence of meibomian gland regeneration and recovery from severe acinar atrophy has been reported in animal models.[5] The findings from these studies were not detected using the high-level semiquantitive review of meibography images. Precision methods, innovated to monitor subtle changes, were found to correlate with meaningful clinical results. As such, the evaluation of subtle morphological changes in meibomian gland structure over short periods of time has both scientific and clinical merit.

As previously stated, it is not known as to what degree meibography identifies the presence of functional acini versus solely capturing structure. This study was not intended to answer this question. The primary objective of this study is more fundamental, which was to investigate whether there is a measurable change in meibomian gland appearance both diurnally and monthly. The measurable changes might correspond to any change in the morphometric parameters of the meibomian glands such as gland length ratio, gland width, gland area, gland intensity (mean grayscale level) and gland tortuosity. In order to measure these changes, custom software was developed. The relationship between meibomian gland structure and function metrics (lipid layer thickness [LLT], non-invasive tear break-up time [NIBUT] and evaporation rate) was also closely investigated.

Key points

- Meibomian gland appearance remains relatively stable when averaged across all glands; however, significant variations emerge when analysed individually, highlighting glandular dynamics over short time frames.
- Understanding meibomian gland activity cycles is crucial for distinguishing between normal and diseased states, shaping diagnostic approaches and treatment strategies for conditions such as meibomian gland dysfunction.
- Meibomian gland metrics, despite their diagnostic potential, exhibit variability influenced by factors such as diurnal patterns and measurement techniques, underscoring the need for refined assessment methods and further research into glandular dynamics.

METHODS

Study design

This was a longitudinal, prospective study where subjects attended 11 study visits over a 5-week period, each lasting between 20 and 90 min. Each subject attended a screening visit to confirm eligibility. On a separate day, subjects were asked to attend the clinic at 09:00 h (±30 min) and then return every 2 h over the course of a 12-h period (09:00–21:00 h, seven visits in total), with each visit lasting approximately 20 min. Subjects then attended three more visits, at weekly intervals at 09:00 h (±30 min). This study was approved by the University Research Ethics Committee of The University of Manchester prior to recruitment. All procedures adhered to the tenets of the Declaration of Helsinki and all subjects provided written informed consent prior to enrolment. A retrospective power analysis was conducted for the width metric, a widely reported parameter in the literature. Based on data from 15 subjects, the analysis yielded 80% power to detect a difference in gland width of approximately one pixel (assuming an alpha of 0.05 and a two-tailed analysis). This corresponds to a 5% change in this parameter, indicating that even with a small group, this study possessed sufficient power to identify subtle changes, thereby affirming the effectiveness of our initial recruitment approach.

Subjects

Inclusion criteria required all subjects to be non-contact lens wearers between 18 and 40 years of age, willing and able to sign a statement of informed consent, to follow the protocol and not to participate in other clinical research for the duration of this study. The subject's optimal spherical equivalent distance refraction was between +1.00 and −2.00 D with cylinder ≥−1.00 DC in each eye to ensure that the subject was able to maintain fixation during crucial measurements. The current study was designed to evaluate meibomian gland changes in a healthy population. The subject was required to score ≤4 points on the Standard Patient Evaluation of Eye Dryness (SPEED) questionnaire to ensure that only non-dry eye patients were enrolled.[10,11] Subjects were not eligible to participate if they had a history of ocular/systemic disorders that would normally contraindicate participation or a history of corneal refractive surgery, cataract surgery, grade 1.5 or greater slit lamp findings (Efron Grading Scale)[12] or another ocular abnormality including MGD or blepharitis (Grade 1.0 or greater), the use of topical ophthalmic medication or had meibomian gland atrophy exceeding 25% in either the lower or upper eyelid, or central gland atrophy exceeding 25%.

Gland atrophy was evaluated objectively by the examiner (KS) at the time of the screening. Furthermore, they were also ineligible if the number of meibomian glands yielding liquid secretion (MGYLS) was ≤6 in either lower eyelid.[13] Pregnant or breastfeeding women were also excluded. Subjects were asked to attend the study visits having not worn eye makeup that day.

Basic clinical assessments

High-contrast, distance logMAR visual acuity and slit lamp biomicroscopy of the ocular surface of each eye were carried out at the beginning and at the end of each visit (white light biomicroscopy at the beginning of the visit, i.e., no fluorescein application or eyelid eversion to exclude any potential impact on the primary outcome of the study). Clinical changes to ocular tissues (corneal infiltrates, conjunctival redness, limbal redness, corneal neovascularisation, epithelial microcysts, corneal oedema, corneal staining, conjunctival staining, papillary conjunctivitis, blepharitis and MGD) were graded to the nearest 0.1 unit using Efron Grading Scales.[12] MGYLS were assessed with the Meibomian Gland Evaluator™ (Johnson & Johnson Vision, jnjvisionpro.com). Lid wiper epitheliopathy was assessed at each eyelid margin: upper and lower, and in both eyes at the end of each visit (end of the day for the diurnal assessment day) to ensure that the repeated eyelid eversion did not cause any damage. Images of the everted eyelids were captured following the instillation of lissamine green dye. These images were then reviewed by an investigator, who noted no significant staining in any of the participants. All procedures were performed by the same examiner (KS).

Meibomian gland assessment

The main clinical assessments were administered sequentially starting with LLT evaluation using the LipiView® II system (Johnson & Johnson Vision, jnjvisionpro.com). Meibography was then performed on both eyelids (upper and lower) using the same device. Next, NIBUT was measured using the Medmont E300 Corneal Topographer (Medmont Pty Ltd., medmont.com.au). The measurement was repeated three times (each at least 30 s apart) and the median value recorded. Finally, tear film evaporation rate was measured with the validated closed-chamber Eye-VapoMeter (Delfin Technologies, delfintech.com). This measurement was repeated three times and the mean recorded. All measurements were taken by the same examiner (KS). LLT, NIBUT and evaporation rate were used as indirect measures of meibomian gland function. These measurements were performed on the right eye only. The left eyelids were used as a reference, to verify whether these clinical measures or the instrumentation used in these additional procedures influenced meibomian gland appearance. For diurnal assessment, the right eye was imaged every 2 h throughout the day. Additionally, the left eye was imaged at baseline, at 09:00 h, and then at the end of the day (21:00 h). Meibomian gland changes were evaluated on two levels; first, the overall changes in aggregated meibomian glands were analysed, with the value averaged across all glands in the eyelid. Then, the changes in individual meibomian glands were analysed, where each gland was treated as a single entity.

Image processing

Captured images were processed using custom semi-automated image analysis software to calculate meibomian gland metrics. Individual meibomian gland labels were selected manually using the interactive tool Image Labeler app provided by MATLAB R2022a (MathWorks, Inc., mathworks.com). The Smart Polygon tool was then used to estimate the shape of each gland individually. The Smart Polygon tool identifies an object of interest by using regional graph-based segmentation ('GrabCut').[14] Estimated regions of interest for individual glands were further corrected with the Brush tool to ensure precise labelling of the gland. Six central glands were selected for each subject; all images were labelled by one annotator (KS) who ensured that the same glands were selected across all visits for each subject. Furthermore, to avoid introducing any error on the surface, geometry or intensity of the analysed glands due to specular reflections, we excluded glands that had a specular reflection at any of the imaging sessions. All images were carefully analysed by the same observer, who examined all images for each subject from all visits and decided which glands would be included in the analysis. The following meibomian gland metrics were developed to quantify changes over time: Meibomian gland length, length ratio, area, intensity, tortuosity and width. Meibomian gland length was

defined as the pixel-wise length of the gland topological skeleton.[15] Length ratio was the length of the gland with respect to eyelid height at the position of the gland (see Figure 1) and was introduced to compensate for changes in the angles of the eyelid in relation to the camera.[16] Individual meibomian gland area was defined as the number of pixels within each gland. Meibomian gland intensity was defined as the mean grey level of each labelled gland (the brightness of all pixels within a single gland, range 0–255). In order to standardise the pixel intensity across all images, we used a reference image taken at the first visit. The same imaging device was used throughout the study, in the same room by the same operator. To account for any potential variation in lighting conditions, we also ensured that the window blinds were closed for each imaging session. The pixel intensity of each image was calibrated using custom MATLAB software that we developed. This software applied morphological dilation to binary gland masks and subtracted dilated gland margin masks from dilated background masks to determine the intensity in the region. By comparing the intensity of gland regions in the reference image to that in subsequent images and adjusting the intensity of the subsequent images accordingly, we ensured that pixel intensity remained consistent across all images, even if the lighting conditions varied between visits. Tortuosity was defined as the ratio of the arc-length of the gland (length of the curve or length of gland topological skeleton) to the distance between the end points (see Figure 3).[15] Meibomian gland width was calculated as the average of all widths of the gland along all points on the gland central line, similar to the definition of Xiao et al.[17] Using principal component analysis (PCA), the perpendicular direction to the gland's topological skeleton

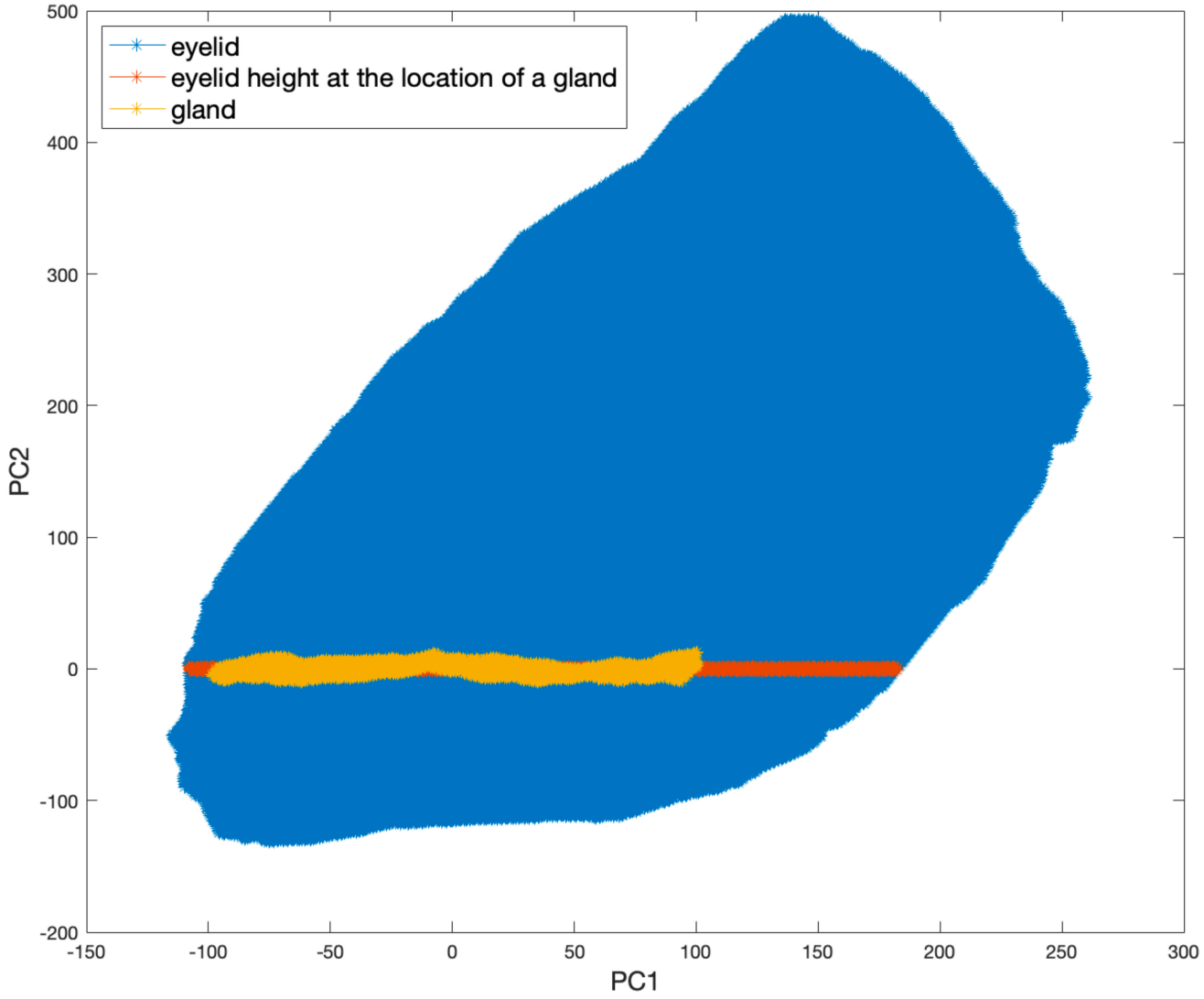

FIGURE 1 Meibomian gland ratio calculation. Blue colour represents the eyelid, orange represents the height of the eyelid at the position of the gland and yellow corresponds to the gland of interest. This image represents a rotated object after performing principal component analysis (PCA) on the data. PC1 (principal component 1) and PC2 (principal component 2) are the two most important axes of the rotated object, with PC1 representing the direction of the greatest variability in the data and PC2 representing the direction of the second-greatest variability. The values along PC1 and PC2 can be used to describe the object's shape and orientation.

was calculated for each point along the gland. This allowed us to compensate for gland curvature and measure the width as the actual distance between the gland contours (see Figure 2). Meibomian gland width was measured perpendicular to the skeleton at all points along the gland, and the mean, median, 10th and 90th percentile widths were calculated to provide comprehensive information about gland structure and function. The median was determined to deal with potential outliers, while the 10th and 90th percentiles were introduced to detect a potential change in the thinnest and thickest regions, respectively.

Statistical analysis

All data summaries and statistical analyses were performed using SAS software Version 9.4 (sas.com). Descriptive statistics were reported for all key variables as appropriate. Continuous data were summarised descriptively by *n*, mean, standard deviation (SD), median, minimum (Min) and maximum (Max). Categorical data were summarised descriptively by frequency count (*n*) and percentage (%) of subjects or eyes within each category level. Summaries were presented by visit, as applicable, for the analysis population set of interest. The denominator for all percentages was the number of subjects (or eyes as applicable) with available data in the group under consideration.

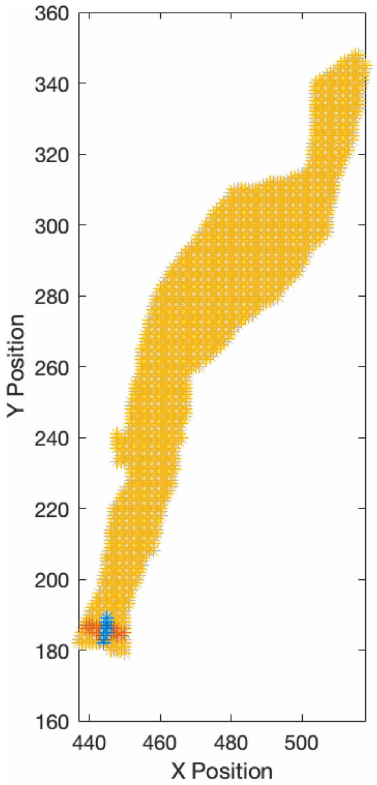

FIGURE 2 Meibomian gland width calculation using principal component analysis (PCA). The perpendicular direction (marked in red) to the gland's topological skeleton is calculated for each point using PCA of eight neighbouring points (marked in blue). Meibomian gland widths were measured perpendicular to the gland's skeleton at all points and were then used to calculate the mean, median, 10th and 90th percentile widths, providing a comprehensive understanding of the gland's structure and function.

Least-square (LS) means were used to estimate the mean value for each factor level in the linear mixed-effects models used for statistical analysis. LS means can provide more accurate estimates of group means compared with raw means, as they account for differences in the number of observations and variance within and between groups. LS means were calculated by adjusting the raw means using a statistical model that included all the factors and covariates in the analysis.

Meibomian gland metrics were analysed using a linear mixed model to compare the differences at various time points. Time point and eyelid location (lower and upper) were included as fixed effects. Age and sex were also included as fixed covariates. The subject was included as a random effect. A compound symmetry was chosen to model the residual errors between repeated measurements of meibomian gland metrics within the same subject, subject's eyes and same visit across the subject's eyelids. Statistical difference was concluded if the lower confidence limit of the least-square mean differences was greater than zero or the upper limit was less than zero. For evaporation rate, a log-normal distribution was chosen for a better fit to the residual, and the statistical difference was concluded if lower confidence limit of the least-square mean ratios was greater than one or the upper limit was less than one. To counteract the multiple comparisons for meibomian gland metrics, a Bonferroni-corrected *p*-value was used.

To help illustrate the variation in measures which could be expected due to intra-observer repeatability, 10 measures were recorded for a single test subject for which coefficients of repeatability were determined using the method described by Bland and Altman,[18] where the coefficient of reliability is defined as 2.77 times the within-subject standard deviation (Sw). The Wilson method for calculating confidence intervals for proportions was used to calculate the lower and upper limits of the 95% confidence intervals for the proportion of glands that lay outside the lines set by the coefficient of repeatability for each metric.[19]

In order to assess changes on an individual gland basis, the percentage of glands that lay outside the lines set by the coefficient of repeatability for each metric was calculated. If the number of points outside the coefficient of repeatability lines was >5%, then it was assumed that the change was statistically significant.

RESULTS

Demographics

A total of 15 participants (8 [53%] females and 7 males) were enrolled in the study, with 13 identifying as White, one as Latino and one as South Asian. Ethnicity information was

$$MG\ tortuosity = \frac{Arclength}{Distance\ between\ endpoints}$$

FIGURE 3 Meibomian gland tortuosity calculation.

self-reported by the participants. The mean age of the study participants was 21.9 ± 2.5 years, ranging from 19 to 27 years. One participant did not complete the study (missed two final visits) and another missed one afternoon visit (17:00 h) during the diurnal meibomian gland assessment day.

Diurnal variations in meibomian gland structure and function

Aggregate meibomian gland change

None of the meibomian gland structural metrics were significantly influenced by the time of the visit. Figure S1 shows the least-square mean (LSM) differences from baseline for changes in meibomian gland metrics throughout the day for both the upper and lower eyelids. The mixed model demonstrated a significant effect of eyelid location (upper and lower) on all metrics: with area ($F = 156.55$, $p < 0.0001$), length ratio ($F = 19.34$, $p < 0.0001$) and intensity ($F = 694.44$, $p < 0.0001$) greater for the upper eyelid while tortuosity ($F = 286.77$, $p < 0.0001$), $width_{mean}$ ($F = 889.84$, $p < 0.0001$), $width_{median}$ ($F = 1891.49$, $p < 0.0001$), $width_{10th}$ ($F = 722.81.74$, $p < 0.0001$) and $width_{90th}$ ($F = 1041.55$, $p < 0.0001$) were greater for the lower eyelid. There was no effect of time point on the differences between the eyes (right and left) for any of the metrics.

There was a significant effect of time on LLT ($F = 6.22$, $p < 0.0001$), with LLT for the 19:00 h (mean difference [95% confidence interval]): (−10.87 [−20.83, −0.92] nm) and 21:00 h (−12.87 [−22.91, −2.82] nm) visits being significantly thinner than that of the 09:00 h baseline (Figure 4). Time of the visit had no effect on NIBUT ($F = 0.81$, $p = 0.60$, see Figure 5) and evaporation rate ($F = 0.90$, $p = 0.53$, see Figure 6).

Individual meibomian gland change

Figure S2 shows the differences in meibomian gland metrics across a day when each gland was considered individually. Table 1 shows the corresponding percentage of values that were either higher or lower than the values set by the coefficients of repeatability.

Monthly variations in meibomian gland structure and function

Aggregate meibomian gland change

Figure S3 shows the LSM differences from baseline for changes in meibomian gland metrics over a month for both the upper and lower eyelids.

There was a significant effect of time on LLT ($F = 6.22$, $p < 0.0001$), with LLT at Week 2 being significantly thicker by 11.32 (1.13, 21.50) nm than that at the Week 1 baseline. Figures 7–9 show the absolute values of LLT, NIBUT and evaporation rate and the differences for each from baseline.

Individual meibomian gland change

Figure S4 shows the differences in meibomian gland metrics across a month when each gland was considered individually. Table 1 shows the corresponding percentage of values that were either higher or lower than the values set by coefficients of repeatability.

Correlation between meibomian gland structure and function metrics

Correlations between meibomian gland appearance metrics and meibomian gland function metrics for the upper and lower eyelids of the right eye, respectively, are shown in Tables 2 and 3. The Bonferroni-corrected p-value was 0.001 (the number of analyses on the dependent variable = 48). There was no significant correlation between any meibomian gland appearance metrics and meibomian gland function metrics.

DISCUSSION

The main goal of the current study was to determine whether there was a measurable change in meibomian gland appearance over short periods of time, specifically at 12 h and 4 weeks. To our knowledge, this is the first study to undertake a longitudinal analysis of meibomian gland appearance changes over such short time frames. The results of this investigation show that generally, meibomian gland structure does not change when all glands were evaluated en masse, that is, averaging across all glands for each eyelid. However, when looking at the results on a gland by gland basis, some metrics showed significant variation over time both diurnally and monthly.

It is generally known that not all glands are in operation simultaneously.[20] For example, Norn showed that approximately 45% glands were active at any one time.[21] Furthermore, Korb and Blackie noted that gland

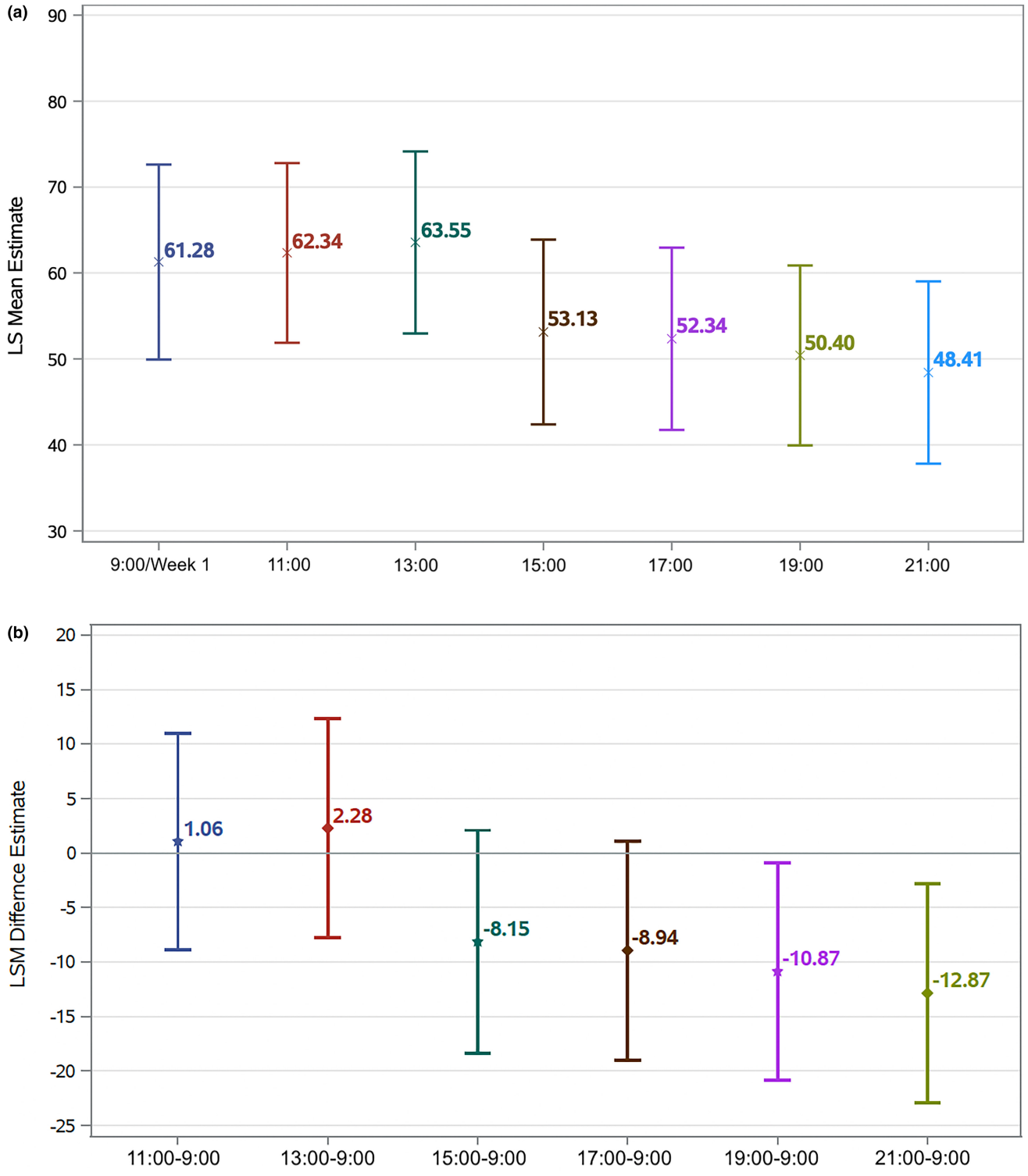

FIGURE 4 Diurnal changes in lipid layer thickness. (a) Least-square (LS) means for changes in lipid layer thickness throughout the day (expressed in nm). (b) Least-square mean (LSM) differences from baseline for changes in lipid layer thickness throughout the day (expressed in nm).

activity varied across the lower eyelid, as the majority of active glands were found in the nasal third of the eyelid while the least activity was found in the temporal third.[13] The number of active glands was found to be around six, with a tendency to decrease as dry eye symptoms progressed.[13]

A further interesting finding regarding gland activity was observed by the same research group. A study focused on the time needed for a meibomian gland to be drained and the recovery time needed to express lipids again after full drainage.[22] It was observed that a single central gland can be drained within 8–20 s and it took

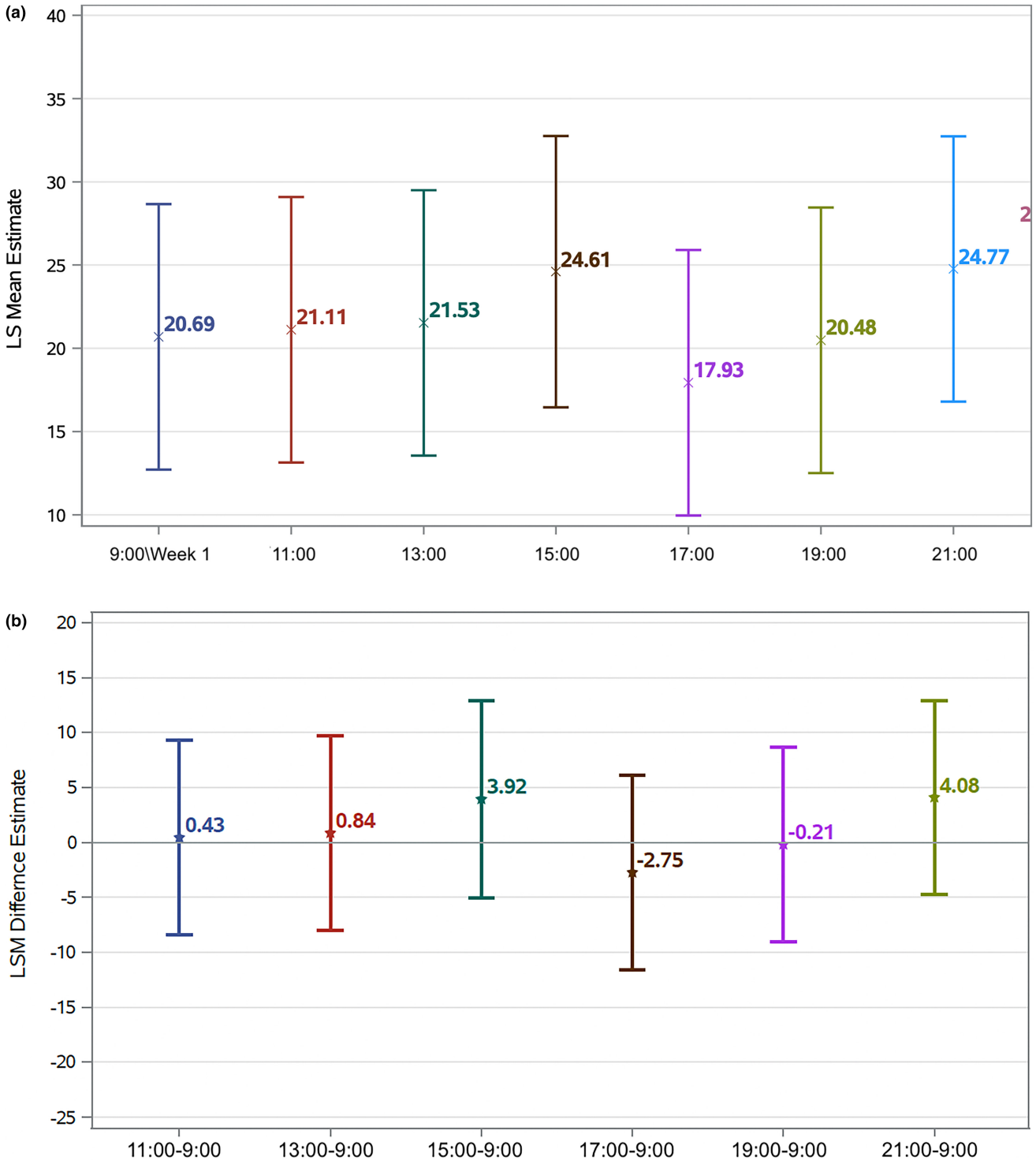

FIGURE 5 Diurnal changes in non-invasive break-up time. (a) Least-square (LS) means for changes of non-invasive break-up time throughout the day (expressed in seconds). (b) Least-square mean (LSM) differences from baseline for changes of non-invasive break-up time throughout the day (expressed in seconds).

over 2 h for the gland to partially recover and secrete lipids again.[22] In addition, Blackie and Korb demonstrated diurnal secretory characteristics of individual meibomian glands.[23] They showed that a single gland is capable of continuous lipid secretion over 9 h. Moreover, the likelihood of secretion on demand varies across the eyelid as 69% of tested glands within the nasal third were secreting lipids at each measurement (four times a day; 3-h intervals) compared with only 31% and 22% of the central and temporal thirds, respectively.[23] These findings have a number of practical implications. A full understanding of individual gland function in a young, healthy population

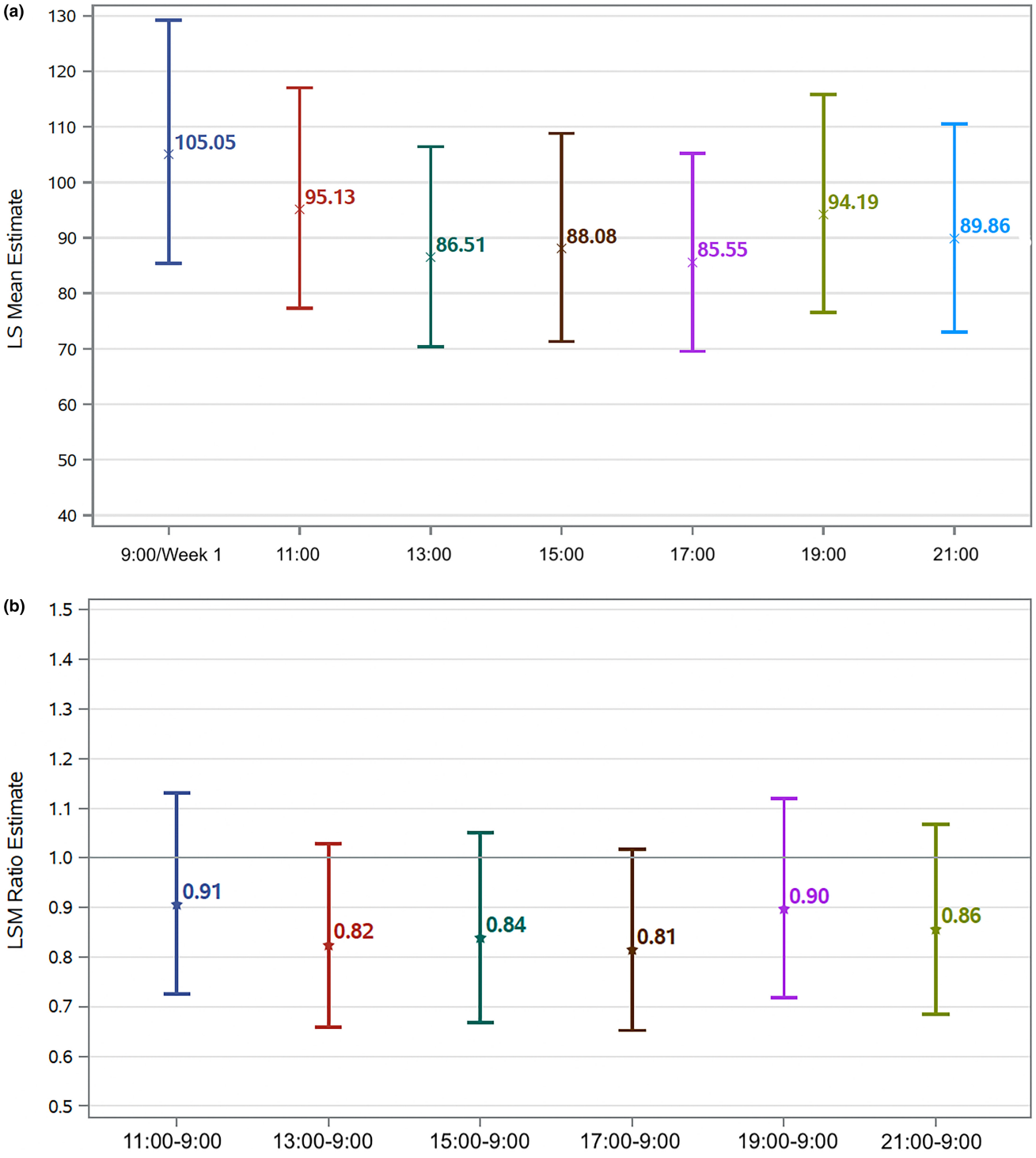

FIGURE 6 Diurnal changes in evaporation rate. (a) Least-square (LS) means for changes in evaporation rate throughout the day (expressed in g/m^2/h). (b) Least-square means (LSM) ratios for changes in evaporation rate throughout the day (ratio unitless).

can provide the groundwork for understanding changes in gland secretion in MGD. Meibomian glands undergo a cycle of activity, which means that not all glands are active at the same time. During the gland's inactive phase, it is difficult to distinguish between a gland in a resting state and one in a diseased state. Thus, a gland may not be active because of its normal cycle or due to a disease that affects its ability to produce lipids. Therefore, it is important to consider the stage of the gland's activity cycle when evaluating meibomian gland function and appearance.[24]

Looking from a different perspective, as noted by Blackie and Korb, warm compresses used as an eyelid treatment might be less effective than previously thought

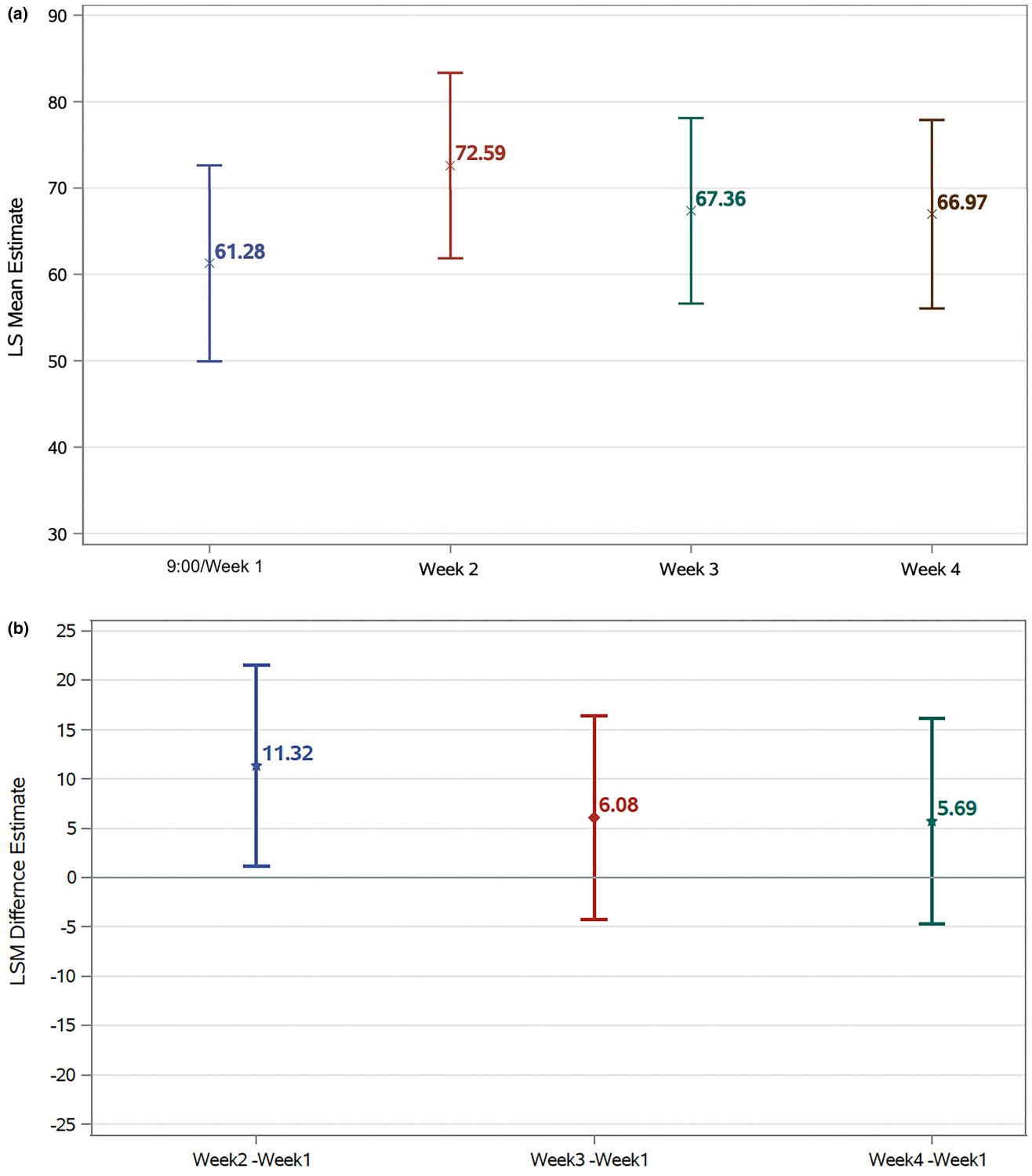

FIGURE 7 Monthly changes in lipid layer thickness. (a) Least-square (LS) means for changes in lipid layer thickness throughout the month (expressed in nm). (b) Least-square means (LSM) differences from baseline for changes in lipid layer thickness throughout the month (expressed in nm).

because gland drainage could cause a counterproductive response resulting in discomfort sometime after treatment.[23] The results of the present study provide additional evidence with respect to the meibomian gland cycle of activity. While the overall performance of a set of meibomian glands remains more or less constant, this cannot be generalised to an individual gland. A change in individual meibomian gland appearance may be related to the meibocyte cycle. A study on rats has shown that cells migrate from the basement membrane towards the centre of the acinus (approximately 0.6 μm/day). The basal layer of meibocytes acts as a proliferating progenitor which

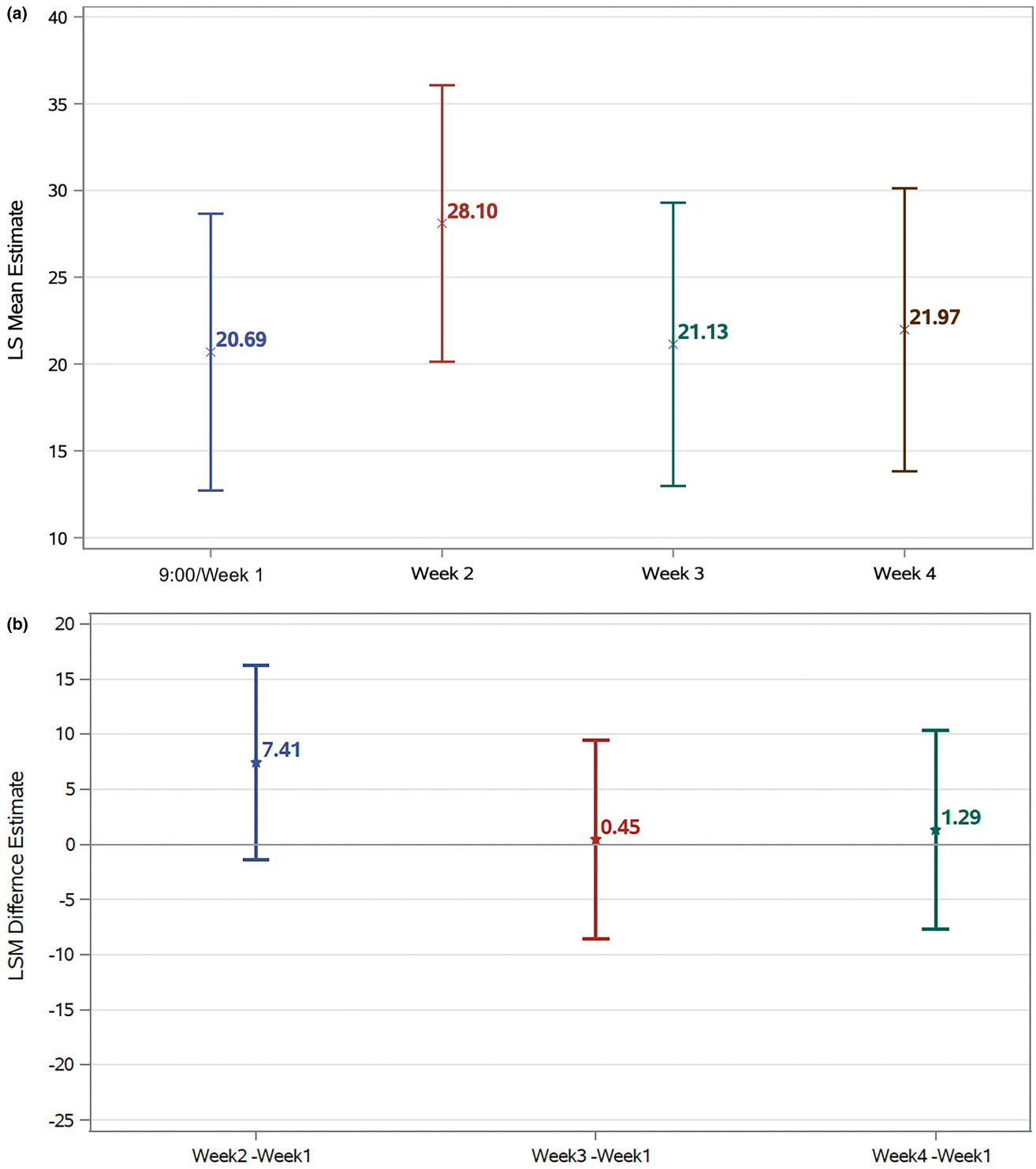

FIGURE 8 Monthly changes in non-invasive break-up time. (a) Least-square (LS) means for changes in non-invasive break-up time throughout the month (expressed in seconds). (b) Least-square mean (LSM) differences from baseline for changes of non-invasive break-up time throughout the month (expressed in seconds).

generates new meibocytes every 4 days,[25] which differentiates through the acinus. Furthermore, according to Olami et al.,[25] undifferentiated cells are located at the periphery of the acinus and it takes approximately 9 days for differentiating cells to migrate towards the centre of the acinus where the totally differentiated cells are located. Olami et al.[25] explained the constant secretion of meibum by identifying the movement of descendant meibocytes. These movements, together with mechanical forces at each blink, which implicate the muscular action of the orbicularis and Riolan's muscle, are responsible for the delivery of meibum into the orifice.[26]

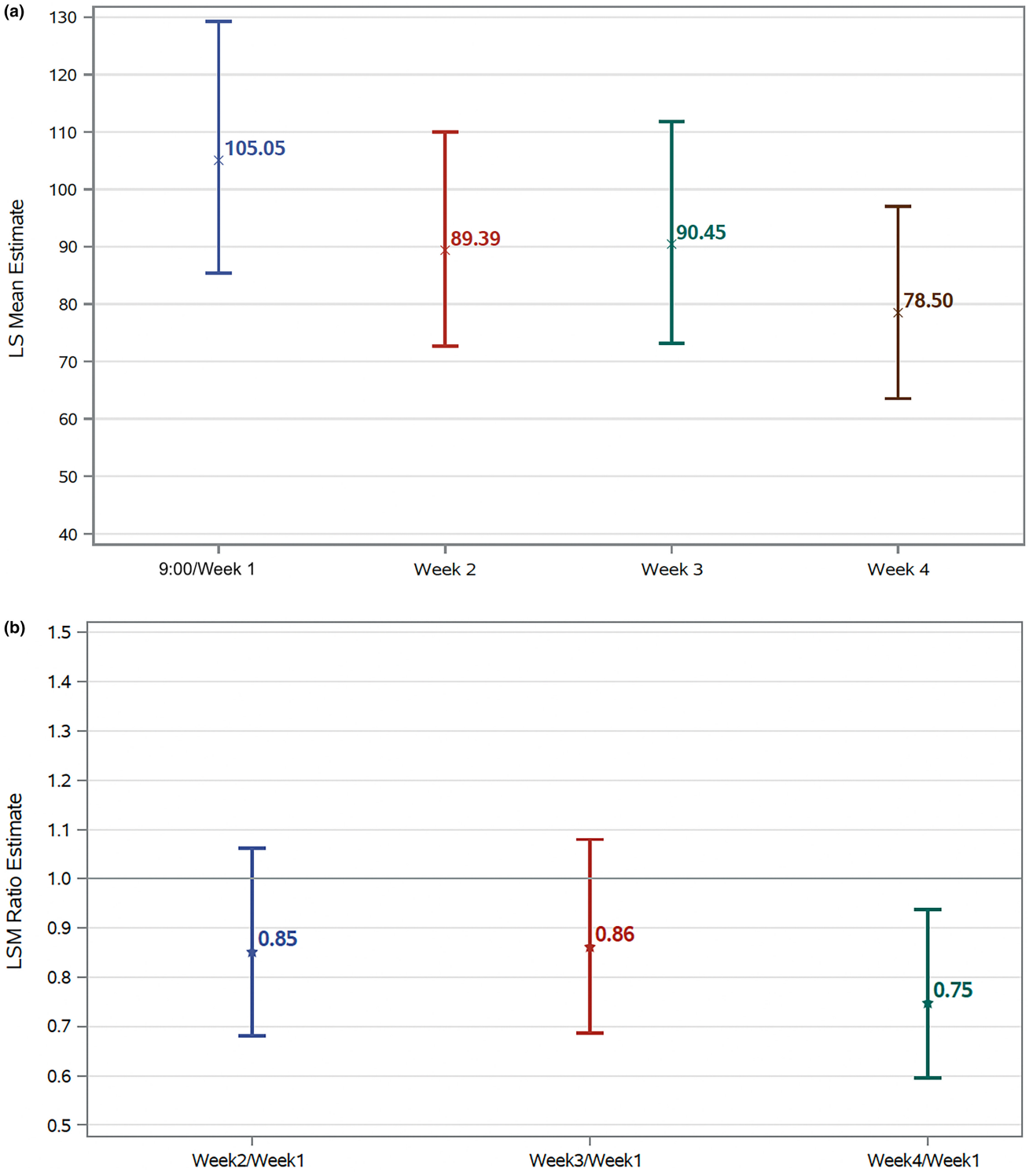

FIGURE 9 Monthly changes in evaporation rate. (a) Least-square (LS) means for changes in evaporation rate throughout the month (expressed in g/m^2/h). (b) Least-square mean (LSM) ratios for changes in evaporation rate throughout the month (ratio unitless).

The diagnostic capability of many meibomian gland metrics has been comprehensively described.[27] Even though the objective analysis of meibography images is still a developing field, there is some tentative initial evidence that overall meibomian gland appearance correlates with ocular function parameters such as bulbar redness, foam secretion, conjunctival staining and fluorescein break-up time (FBUT).[28] Tear break-up time has received the most interest out of these parameters. It has been shown that FBUT is positively correlated with meibomian gland width, length ratio and irregularity.[28] Similarly, Pult et al.[29] found that meibomian gland tortuosity and the width of the

TABLE 1 Percentage (95% CI) of glands outside the lines set by the coefficient of repeatability for each metric.

	Length ratio	Area	Intensity	Tortuosity	$Width_{mean}$	$Width_{median}$	$Width_{10th}$	$Width_{90th}$
Upper eyelid diurnal	**7.12** (5.23,9.62)	**23.6** (20.20, 27.38)	0.94 (0.40, 2.18)	4.12 (2.74, 6.16)	**13.86** (11.19, 17.05)	**8.24** (6.20, 10.88)	1.12 (0.51, 2.42)	**6.93** (5.07, 9.41)
Monthly	6.20 (4.45, 8.57)	**20.54** (17.33, 24.17)	1.55 (0.80, 3.00)	5.04 (3.48, 7.24)	**11.24** (8.83, 14.20)	**7.00** (5.13, 9.49)	1.55 (0.80, 3.00)	4.26 (2.85, 6.32)
Lower eyelid diurnal	**10.86** (8.50, 13.78)	3.93 (2.58, 5.93)	1.69 (0.89, 3.18)	**8.99** (6.85, 11.72)	**25.66** (22.14, 29.53)	**17.60** (14.60, 21.06)	**24.91** (21.43, 28.75)	**7.68** (5.71, 10.25)
Monthly	**9.3** (7.12, 12.06)	4.26 (2.85, 6.32)	0.78 (0.31, 1.95)	**9.30** (7.12, 12.06)	**22.87** (19.51, 26.62)	**19.78** (16.62, 23.37)	**23.64** (20.23, 27.42)	5.81 (4.12, 8.13)

Note: Values in bold indicate metrics for which the number of data points outside the coefficient of repeatability was definitely greater than 5%.

upper eyelid glands were significantly correlated with NIBUT. However, these results do not align with those presented here, as none of the subjects in this study had ocular surface disease or symptoms of discomfort, and different metrics and measuring processes were used. Building on these insights, it is noteworthy that Singh et al.[30] delved into the histopathological features of various morphological variants of meibomian glands. Their research revealed that the dark areas on meibography, indicative of meibomian gland dropout, lack residual glandular structure upon histological examination. This compelling evidence highlighted diverse morphological changes within the meibomian glands, alluding to the intriguing observation that these alterations do not necessarily translate into significant functional consequences. Importantly, the majority of the morphological changes were not linked to crucial functional alterations, except for the instance of short glands, which exhibited atrophic changes characterised by a loss of meibocyte differentiation and cellular proliferation.[30]

The secondary aim of this study was to examine whether there were any substantial changes in the LLT, NIBUT and tear film evaporation rate within a day (12 h) and a month. The results demonstrated that NIBUT and evaporation rate did not exhibit significant changes over the course of a day or a month. Conversely, LLT decreased gradually as the day progressed. It has been reported previously that these parameters can vary throughout the day.[31–38] The evaporation rate tends to be lowest after awakening and highest 2 h after awakening and then it reaches a plateau.[31] In contrast, Arroyo et al. showed that the tear evaporation rate had no significant variability over the course of a day.[32] In addition, Wojtowicz and McCulley[33] highlighted that measurements should be taken in the afternoon rather than in the morning, as the evaporation rate showed less variability at this later time of the day. TBUT may reduce at the end of the day.[34] However, other studies found no changes as the day progressed.[32,35–37] Dry eye patients tend to have a longer NIBUT in the morning than at the end of the day.[35]

The findings in this report are subject to at least four limitations. First, the current study had a small sample size, which reflected the exploratory nature of the investigation. Second, a source of uncertainty that could have affected the measurement of meibomian gland metrics was the subjective and manual process of annotating the images. Even though the images were labelled by a single masked annotator, it was still a subjective matter to distinguish between gland and eyelid regions. A more reliable and objective method of image segmentation is needed. There are a number of published examples that used artificial intelligence-based algorithms to perform meibomian gland image segmentation in an objective, repeatable and reliable way.[15,39–44] Third, there is the possibility of measurement errors in the calculation of meibomian gland intensity. Since the manner in which the LipiView® processes images is proprietary, we cannot affirm that the measurements captured at different time points reflect actual changes or induced differences

TABLE 2 Pearson correlation coefficients and *p*-values for the upper eyelid metrics of the right eye.

	Length ratio	Area	Intensity	Tortuosity	$Width_{mean}$	$Width_{median}$	$Width_{10th}$	$Width_{90th}$
LLT	−0.0667	−0.2527	−0.0252	−0.1178	−0.231	−0.2332	−0.0841	−0.288
	0.4459	*0.0033*	*0.7731*	*0.1771*	*0.0075*	*0.0069*	*0.3359*	*0.001*
NIBUT	*0.0244*	−0.0634	−0.1243	−0.2432	−0.1313	−0.1242	−0.0374	−0.1716
	0.7689	*0.4453*	*0.1335*	*0.003*	*0.1129*	*0.1337*	*0.6525*	*0.0377*
Evaporation rate	−0.0983	−0.0347	0.0761	0.2434	0.0399	−0.0138	−0.0254	0.1335
	0.2361	*0.6766*	0.3596	*0.003*	*0.6314*	*0.8683*	*0.7603*	*0.1069*

Note: Number of observations = 133 (LLT) and 147 (NIBUT and evaporation rate). 10th and 90th refer to the respective percentiles. The italic values indicate the Bonferroni-corrected *p*-value was 0.001 (the number of analyses on the dependent variable = 48).

Abbreviations: LLT, lipid layer thickness; NIBUT, non-invasive break-up time.

TABLE 3 Pearson correlation coefficients and *p*-values for the lower eyelid metrics of the right eye.

	Length ratio	Area	Intensity	Tortuosity	$Width_{mean}$	$Width_{median}$	$Width_{10th}$	$Width_{90th}$
LLT	0.0095	0.024	0.1746	−0.2597	−0.1302	−0.1561	−0.0913	−0.0848
	0.2762	*0.7841*	*0.0445*	*0.0025*	*0.1354*	*0.0727*	*0.2961*	*0.3318*
NIBUT	0.2396	0.064	−0.0678	−0.037	0.1121	0.0828	0.1449	0.098
	0.0035	*0.4414*	*0.4143*	*0.6561*	*0.1763*	*0.3189*	*0.0798*	*0.2356*
Evaporation rate	0.0013	0.0633	0.2474	−0.0224	−0.0095	0.9945	0.0725	−0.0431
	0.988	*0.4459*	*0.0025*	*0.7881*	*0.9091*	*0.7564*	*0.383*	*0.604*

Note: Number of observations = 133 (LLT) and 147 (NIBUT and Evaporation rate). 10th and 90th refer to the respective percentiles. The italic values indicate the Bonferroni-corrected *p*-value was 0.001 (the number of analyses on the dependent variable = 48).

Abbreviations: LLT, lipid layer thickness; NIBIT, non-invasive break-up time.

caused by image processing/enhancement. Finally, the coefficient of repeatability was calculated for only one subject, which could be considered a weakness and could have affected the interpretation of significant changes in meibomian gland structure. However, since the reference variance was much lower than that for the study subjects, the calculation of the coefficient of repeatability for subject 0 is justified. Despite these limitations, the study adds to our understanding of the complicated nature of the meibomian glands.

This research raises many questions in need of further investigation. The meibomian glands do indeed demonstrate measurable variability over short periods of time, but we do not know whether or not they are diurnal. We also do not know whether the glands interact with each other. The data presented here demonstrated that normal meibomian gland morphology is dynamic and subject to measurable change over short time periods such as the course of a day. The clinical implications of this research will be revealed as we improve our ability to assess and interpret meibomian gland morphology as captured with meibography.

AUTHOR CONTRIBUTIONS

Kasandra Swiderska: Conceptualization (equal); data curation (equal); formal analysis (equal); investigation (lead); methodology (equal); software (equal); validation (lead); visualization (lead); writing – original draft (lead). **Caroline A. Blackie:** Conceptualization (equal); data curation (equal); formal analysis (equal); funding acquisition (equal); investigation (equal); methodology (equal); resources (equal); supervision (equal); writing – review and editing (equal). **Carole Maldonado-Codina:** Conceptualization (equal); data curation (equal); formal analysis (equal); funding acquisition (equal); investigation (equal); methodology (equal); resources (equal); supervision (equal); writing – review and editing (equal). **Martin Fergie:** Conceptualization (equal); data curation (equal); formal analysis (equal); investigation (equal); methodology (equal); resources (equal); software (equal); supervision (equal); validation (equal); visualization (equal); writing – review and editing (equal). **Michael L. Read:** Conceptualization (equal); data curation (equal); formal analysis (equal); funding acquisition (equal); investigation (equal); methodology (equal); resources (equal); supervision (equal); validation (equal); visualization (equal); writing – review and editing (equal). **Philip B. Morgan:** Conceptualization (equal); data curation (equal); formal analysis (equal); funding acquisition (equal); investigation (equal); methodology (equal); resources (equal); supervision (equal); validation (equal); visualization (equal); writing – review and editing (equal).

ACKNOWLEDGEMENTS

The authors acknowledge the assistance of our clinical, logistical and administrative colleagues at Eurolens Research in the acquisition of data for this study.

CONFLICT OF INTEREST STATEMENT

The authors declare that they have no known competing financial interests or personal relationships that could have appeared to influence the work reported in this paper. The article results from research sponsored by Johnson and Johnson Vision, Inc. (C. Blackie is an employee of Johnson and Johnson Vision, Inc.). The terms of this arrangement have been reviewed and approved by The University of Manchester in accordance with its conflict of interest policies.

ORCID

Kasandra Swiderska https://orcid.org/0000-0002-1638-2141
Caroline A. Blackie https://orcid.org/0000-0002-4618-3303
Carole Maldonado-Codina https://orcid.org/0000-0002-4101-376X
Michael L. Read https://orcid.org/0000-0002-9976-8567
Philip B. Morgan https://orcid.org/0000-0003-0680-8169

REFERENCES

1. Jester JV, Rife L, Nii D, Luttrull JK, Wilson L, Smith RE. In vivo biomicroscopy and photography of meibomian glands in a rabbit model of meibomian gland dysfunction. *Invest Ophthalmol Vis Sci*. 1982;22:660–7.
2. Arita R, Suehiro J, Haraguchi T, Maeda S, Maeda K, Tokoro H, et al. Topical diquafosol for patients with obstructive meibomian gland dysfunction. *Br J Ophthalmol*. 2013;97:725–9.
3. Hura A, Epitropoulos A, Blackie CA, Davis (McClelland) T. The potential effect of lipiflow on meibomian gland structure: a preliminary analysis utilizing dynamic meibomian imaging. *Invest Ophthalmol Vis Sci*. 2018;59:ARVO E-Abstract 935.
4. Hura AS, Epitropoulos AT, Czyz CN, Rosenberg ED. Visible meibomian gland structure increases after vectored thermal pulsation treatment in dry eye disease patients with meibomian gland dysfunction. *Clin Ophthalmol*. 2020;14:4287–96.
5. Reneker LW, Yang X, Zhong X, Huang AJW. Meibomian gland (MG) acinar regeneration from atrophy in a Fgfr2 conditional knockout mouse model (abstract). *Invest Ophthalmol Vis Sci*. 2019;60:ARVO E-Abstract 1412.
6. Finis D, König C, Hayajneh J, Borrelli M, Schrader S, Geerling G. Six-month effects of a thermodynamic treatment for MGD and implications of meibomian gland atrophy. *Cornea*. 2014;33:1265–70.
7. Arita R. Meibography: a Japanese perspective. *Invest Ophthalmol Vis Sci*. 2018;59:DES48–ES55.
8. Craig JP, Nichols KK, Akpek EK, Caffery B, Dua HS, Joo CK, et al. TFOS DEWS II definition and classification report. *Ocul Surf*. 2017;15:276–83.
9. Nichols KK, Foulks GN, Bron AJ, Glasgow BJ, Dogru M, Tsubota K, et al. The international workshop on meibomian gland dysfunction: executive summary. *Invest Ophthalmol Vis Sci*. 2011;52:1922–9.
10. Ngo W, Situ P, Keir N, Korb D, Blackie C, Simpson T. Psychometric properties and validation of the standard patient evaluation of eye dryness questionnaire. *Cornea*. 2013;32:1204–10.
11. Hashmani N, Munaf U, Saleem A, Javed SO, Hashmani S. Comparing Speed and OSDI questionnaires in a non-clinical sample. *Clin Ophthalmol (Auckland, NZ)*. 2021;15:4169–73.
12. Efron N. Grading scales for contact lens complications. *Ophthalmic Physiol Opt*. 1998;18:182–6.
13. Korb DR, Blackie CA. Meibomian gland diagnostic expressibility: correlation with dry eye symptoms and gland location. *Cornea*. 2008;27:1142–7.
14. Rother C, Kolmogorov V, Blake A. Grabcut—interactive foreground extraction using iterated graph cuts. *ACM Trans Graph (SIGGRAPH)*. 2004;23:309–14.
15. Prabhu SM, Chakiat A, Shashank S, Vunnava KP, Shetty R. Deep learning segmentation and quantification of meibomian glands. *Biomed Signal Process Control*. 2020;57:101776. https://doi.org/10.1016/j.bspc.2019.101776
16. Llorens-Quintana C, Rico-del Viejo L, Syga P, Madrid-Costa D, Iskander DR. A novel automated approach for infrared-based assessment of meibomian gland morphology. *Transl Vis Sci Technol*. 2019;8:17. https://doi.org/10.1167/tvst.8.4.17
17. Xiao P, Luo Z, Deng Y, Wang G, Yuan J. An automated and multiparametric algorithm for objective analysis of meibography images. *Quant Imaging Med Surg*. 2020;11:1586–99.
18. Bland JM, Altman DG. Measuring agreement in method comparison studies. *Stat Methods Med Res*. 1999;8:135–60.
19. Wilson EB. Probable inference, the law of succession, and statistical inference. *J Am Stat Assoc*. 1927;22:209–12.
20. Norn M. Natural fat in external eye. *Acta Ophthalmol*. 1980;58:331–6.
21. Norn M. Meibomian orifices and Marx's line studied by triple vital staining. *Acta Ophthalmol*. 1985;63:698–700.
22. Blackie CA, Korb DR. Recovery time of an optimally secreting meibomian gland. *Cornea*. 2009;28:293–7.
23. Blackie CA, Korb DR. The diurnal secretory characteristics of individual Meibomian glands. *Cornea*. 2010;29:34–8.
24. Tomlinson A, Bron AJ, Korb DR, Amano S, Paugh JR, Pearce EI, et al. The international workshop on meibomian gland dysfunction: report of the diagnosis subcommittee. *Invest Ophthalmol Vis Sci*. 2011;52:2006–49.
25. Olami Y, Zajicek G, Cogan M, Gnessin H, Pe'er J. Turnover and migration of meibomian gland cells in rats' eyelids. *Ophthalmic Res*. 2001;33:170–5.
26. Linton RG, Curnow DH, Riley WJ. The meibomian glands: an investigation into the secretion and some aspects of the physiology. *Br J Ophthalmol*. 1961;45:718–23.
27. Swiderska K, Read ML, Blackie C, Maldonado-Codina C, Morgan PB. Latest developments in meibography: a review. *Ocul Surf*. 2022;25:119–28.
28. Llorens-Quintana C, Rico-Del-Viejo L, Syga P, Madrid-Costa D, Iskander DR. Meibomian gland morphology: the influence of structural variations on gland function and ocular surface parameters. *Cornea*. 2019;38:1506–12.
29. Pult H, Riede-Pult BH, Nichols JJ. Relation between upper and lower lids' meibomian gland morphology, tear film, and dry eye. *Optom Vis Sci*. 2012;89:E310–E315.
30. Singh S, Naidu GC, Vemuganti G, Basu S. Morphological variants of meibomian glands: correlation of meibography features with histopathology findings. *Br J Ophthalmol*. 2021;107:195–200.
31. Tomlinson A, Cedarstaff TH. Diurnal variation in human tear evaporation. *J Br Contact Lens Assoc*. 1992;15:77–9.
32. Arroyo CAD, Byambajav M, Fernández I, Martin E, González-García MJ, López-Miguel A, et al. Diurnal variation on tear stability and correlation with tear cytokine concentration. *Cont Lens Anterior Eye*. 2022;45:101705. https://doi.org/10.1016/j.clae.2022.101705
33. Wojtowicz JC, McCulley JP. Assessment and impact of the time of day on aqueous tear evaporation in normal subjects. *Eye Contact Lens*. 2009;35:117–9.
34. Lira M, Oliveira MECR, Franco S. Comparison of the tear film clinical parameters at two different times of the day. *Clin Exp Optom*. 2011;94:557–62.
35. Bitton E, Keech A, Jones L, Simpson T. Subjective and objective variation of the tear film pre-and post-sleep. *Optom Vis Sci*. 2008;85:740–9.
36. Walker PM, Lane KJ, Ousler GW III, Abelson MB. Diurnal variation of visual function and the signs and symptoms of dry eye. *Cornea*. 2010;29:607–12.
37. Pena-Verdeal H, García-Resúa C, Ramos L, Yebra-Pimentel E, Giráldez MJ. Diurnal variations in tear film break-up time determined in

healthy subjects by software-assisted interpretation of tear film video recordings. *Clin Exp Optom*. 2016;99:142–8.
38. Finis D, Pischel N, Borrelli M, Schrader S, Geerling G. Factors influencing the measurement of tear film lipid layer thickness with interferometry. *Klin Monbl Augenheilkd*. 2014;231:603–10.
39. Wang J, Yeh TN, Chakraborty R, Yu SX, Lin MC. A deep learning approach for meibomian gland atrophy evaluation in meibography images. *Transl Vis Sci Technol*. 2019;8:37. https://doi.org/10.1167/tvst.8.6.37
40. Setu MAK, Horstmann J, Stern ME, Steven P. Automated analysis of meibography images: comparison between intensity, region growing and deep learning-based methods. *Ophthalmologe*. 2019;116(Suppl 2):25–218. https://doi.org/10.1007/s00347-019-0940-0
41. Yeh CH, Yu SX, Lin MC. Meibography phenotyping and classification from unsupervised discriminative feature learning. *Transl Vis Sci Technol*. 2021;10:4. https://doi.org/10.1167/tvst.10.2.4
42. Setu MAK, Horstmann J, Schmidt S, Stern ME, Steven P. Deep learning-based automatic meibomian gland segmentation and morphology assessment in infrared meibography. *Sci Rep-UK*. 2021;11:7649. https://doi.org/10.1038/s41598-021-87314-8
43. Khan ZK, Umar AI, Shirazi SH, Rasheed A, Qadir A, Gul S. Image based analysis of meibomian gland dysfunction using conditional generative adversarial neural network. *BMJ Open Ophthalmol*. 2021;6:e000436. https://doi.org/10.1136/bmjophth-2020-000436
44. Wang J, Li S, Yeh TN, Chakraborty R, Graham AD, Yu SX, et al. Quantifying meibomian gland morphology using artificial intelligence. *Optom Vis Sci*. 2021;98:1094–103.

SUPPORTING INFORMATION

Additional supporting information can be found online in the Supporting Information section at the end of this article.

How to cite this article: Swiderska K, Blackie CA, Maldonado-Codina C, Fergie M, Read ML, Morgan PB. Temporal variations in meibomian gland structure—A pilot study. *Ophthalmic Physiol Opt*. 2024;00:1–16. https://doi.org/10.1111/opo.13321